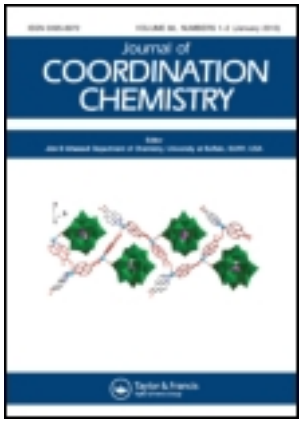

Journal of Coordination Chemistry
Publication details, including instructions for authors and subscription information:
http://www.tandfonline.com/loi/gcoo20

Synthesis, crystal structure, and electrocatalytic behavior of a zinc(II) complex derived from a heterocyclic acylpyrazolone

Xiao-Zhe Pang [a], Jin-Zhou Li [a], Li-Sheng Chen [a] & Heng-Qiang Zhang [b]

[a] College of Chemistry and Chemical Engineering, Harbin Normal University, Harbin, P.R. China

[b] Department of Chemistry, Hebei Normal University for Nationalities, Chengde, P.R. China

Accepted author version posted online: 01 Feb 2013.Published online: 19 Mar 2013.

To cite this article: Xiao-Zhe Pang, Jin-Zhou Li, Li-Sheng Chen & Heng-Qiang Zhang (2013) Synthesis, crystal structure, and electrocatalytic behavior of a zinc(II) complex derived from a heterocyclic acylpyrazolone, Journal of Coordination Chemistry, 66:6, 915-925, DOI: 10.1080/00958972.2013.771775

To link to this article: http://dx.doi.org/10.1080/00958972.2013.771775

Journal of Coordination Chemistry
Vol. 66, No. 6, 20 March 2013, 915–925

Synthesis, crystal structure, and electrocatalytic behavior of a zinc(II) complex derived from a heterocyclic acylpyrazolone

XIAO-ZHE PANG†, JIN-ZHOU LI*†, LI-SHENG CHEN† and HENG-QIANG ZHANG‡

†College of Chemistry and Chemical Engineering, Harbin Normal University, Harbin, P.R. China
‡Department of Chemistry, Hebei Normal University for Nationalities, Chengde, P.R. China

(*Received 8 August 2012; in final form 28 November 2012*)

An acylpyrazolone complex, $[Zn(PM\alpha FP)_2(CH_3OH)_2]$ (HPMαFP = 1-phenyl-3-methyl-4-(α-furoyl)-5-pyrazolone), was synthesized. The complex was characterized by single-crystal X-ray diffraction, IR, UV, fluorescence spectra, DTA-TG, and cyclic voltammetry (CV). The structure is orthorhombic, group pbca with cell parameters: $a = 15.015(3)$ Å, $b = 9.844(2)$ Å, $c = 20.663(4)$ Å, $Z = 4$, $S = 1.025$, $R_1 = 0.0353$ and $wR_2 = 0.0924$. The complex shows a slightly distorted octahedral structure, Zn^{2+} is located at an inversion center from four oxygens, two of ligands in the equatorial plane, two methanols axial. The complex has a two-dimensional supramolecular structure connected by O–H···N bonding interactions. In the CV, one oxidation peak of adenine with $E_p = 1.018$ V in pH = 7.0 shows that the $[Zn(PM\alpha FP)_2(CH_3OH)_2]$/glassy carbon modified electrode has a catalytic effect on adenine.

Keywords: Acylpyrazolone complex; Crystal structure; Spectrum characterization; Electrochemical catalytic; Adenine

1. Introduction

Acylpyrazolone is a *β*-diketone reagent widely used in solvent extractions of metal ions and NMR shift reagents [1–3]. Neutral acylpyrazolones may exist with several possible tautomeric forms. The enol form OH is weakly acidic, as a surfactant, which makes it suitable for electrochemical reactions [4]. Their metal complexes have been found to display catalytic performance, biological activity, and photochromic properties. Pettinari *et al.* reported a review about acylpyrazolones on synthesis, characterization, and coordination chemistry toward a variety of metals and relevant applications [5]. Recently, Jadeja *et al.* have synthesized a toluoylpyrazolone VO^{4+} complex as a catalyst for styrene oxidation [6]. Yang introduced benzoylpyrazolone complexes as biological agents [7]. Jia *et al.* found pyrazolone thiosemicarbazone derivatives which observed the logic behavior of molecular switches [8]. In our previous work, a series of 4-heterocyclic acylpyrazolones and their complexes had

*Corresponding author. Email: lijinzhou20@163.com

ISSN 0095-8972 print/ISSN 1029-0389 online © 2013 Taylor & Francis
http://dx.doi.org/10.1080/00958972.2013.771775

luminiferous and electrochemical character [9–11]. Few attempts have been made on the corresponding Zn(II) complexes. As continuation of this study, we focus on a Zn(II) complex synthesized by solvothermal method, reporting its single crystal structure, spectra (IR, UV, and fluorescence), thermal behavior, and electrochemical properties.

2. Experimental

2.1. *Materials and physical measurements*

HPMαFP was synthesized by the literature procedure [12] (yield: 88%, m.p.: 374–375 K). Anal. Calcd for $C_{15}H_{12}N_2O_3$ (%): C, 66.94; H, 4.43; N, 10.37. Found: C, 67.15; H, 4.52; N, 10.37. Adenine was purchased from Shanghai Reagent Company. All other chemicals used were A.R. quality. C, H, and N elemental analysis were carried out on a Thermo-Fiash EA 1112 elemental analyzer. IR spectra were recorded as KBr pellets on a Bruker Vertex 80 FTIR spectrophotometer. UV–vis spectra were recorded on a Perkin Elmer Lambda 45 spectrophotometer. Thermal analysis was accomplished by a Perkin-Elmer Diamond TG-DTA thermal analyzer. Fluorescence spectra were obtained by a Perkin-Elmer LS55 luminescence spectrophotometer using a 150 W xenon lamp as excitation source. Electrochemical measurements were performed on a CHI-650A electrochemical workstation. A conventional three-electrode system was adopted. The working electrode was a bare or modified glassy carbon electrode (GCE) with a diameter of 3 mm. A platinum wire was used as an auxiliary electrode together with a saturated calomel electrode reference electrode. Stock 1.0×10^{-3} mol L^{-1} adenine solution was prepared in double-distilled water. HPMaFP solution was dissolved in anhydrous ethanol solution. Phosphate buffer solutions (PBS, 0.10 mol L^{-1}) of various pH values were used as supporting electrolytes. All solutions were prepared with double-distilled water and all experiments were conducted at room temperature (298 ± 2 K).

2.2. *Synthesis*

HPMαFP (0.6 mmol, 161 mg) dissolved in 7 mL anhydrous methanol by warming was added dropwise with stirring to a solution of $Zn(CH_3COO_2)_2 \cdot 2H_2O$ (0.3 mmol, 65.85 mg of metal salt in 6 mL anhydrous methanol). The mixture was taken in a 20 mL Teflon-lined stainless steel vessel with addition of a few drops of glacial acetic acid as catalyst, heated to 393 K for 48 h, and then cooled to room temperature over 8 h. Several days later, a large number of yellow crystals were obtained. The product was filtered off, washed several times with anhydrous methanol, and dried in air; yield: 61%. The yellow crystals were recrystallized from DMF and single crystals were obtained at room temperature after several days. m.p.: 440.2–440.5 K. Anal. Calcd for $C_{32}H_{30}O_8N_4Zn$ (%): C, 57.92; H, 4.52; N, 8.45. Found: C, 58.01; H, 4.55; N, 8.51. The reaction procedure is shown in scheme 1.

2.3. *Crystal structure determination and refinement*

A crystal ($0.36 \times 0.22 \times 0.18$ mm^3) was placed on a glass fiber and placed in a Bruker SMART APEX CCD diffractometer with MoKα radiation (0.71073 Å) by using $\omega - \varphi$ scans technique at room temperature. The structure was determined by direct methods with

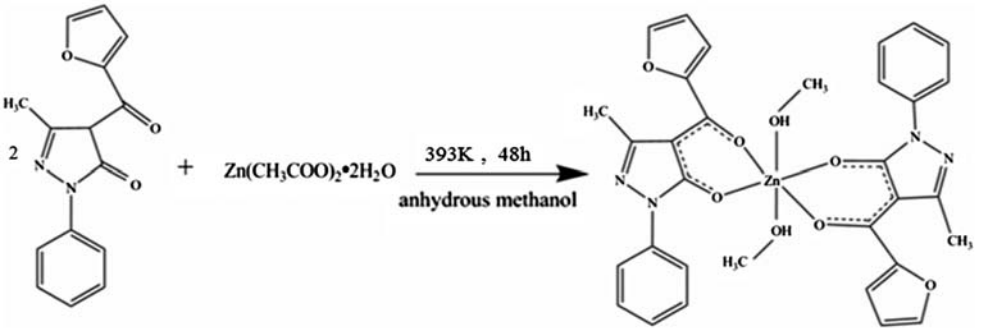

Scheme 1. Synthesis route of $Zn(PM\alpha FP)_2(CH_3OH)_2$.

SHELXS-97 and refined on F^2 using SHELXTL-97 [13]. All non-hydrogen atoms were assigned anisotropic displacement parameters in the refinement. Hydroxyl hydrogens were refined as rigid groups located in a difference Fourier map; other hydrogens were introduced in calculated positions. The parameters of crystal data collection and refinement of the complex are listed in table 1 and selected bond lengths and angles are listed in table 2.

3. Results and discussion

3.1. *Crystal structure*

The structure of the title complex is illustrated in figure 1. The 2D network of the complex is illustrated in figure 2. $[Zn(PM\alpha FP)_2(CH_3OH)_2]$ is six-coordinate Zn(II) with two methanols and four oxygens of two bidentate acylpyrazolonates. The coordination geometry may be described as slightly distorted octahedral. Zn exists in the location of the center of symmetry.

Table 1. Crystal data and structure refinement for the complex.

CCDC	No. 774817
Empirical formula	$C_{32}H_{30}O_8N_4Zn$
Formula weight	663.99
Temperature	295(2) K
Wavelength	0.71073 Å
Crystal system, space group	Orthorhombic, Pbca
Unit cell dimensions	$a = 15.015(3)$ Å, $b = 9.844(2)$ Å, $c = 20.663(4)$ Å $\alpha = 90°$, $\beta = 90°$, $\gamma = 90°$
Volume	3054.3(11) Å^3
Z, Calculated density	4, 2.239 mg/m^3
Absorption coefficient	7.371 mm^{-1}
F(000)	1976
Crystal size	0.36 × 0.22 × 0.18 mm
θ range for data collection	2.66 to 28.31°
Limiting indices	−20<=h<=20, −12<=k<=13, −23<=l<=27
Reflections collected/unique	21,750/3778 [R(int) = 0.0430]
Completeness to theta = 28.31	99.7%
Absorption correction	None
Refinement method	Full-matrix least-squares on F^2
Data/restraints/parameters	3778/1/211
Goodness-of-fit on F^2	1.025
Final R indices [I > 2σ(I)]	$R_1 = 0.0353$, w$R_2 = 0.0924$
R indices (all data)	$R_1 = 0.0615$, w$R_2 = 0.0993$
Largest diff. peak and hole	0.338 and −0.391 eA^{-3}

Table 2. Selected bond lengths (Å) and angles (°) (ESD's are in parentheses).

Selected bond lengths (Å)			
N(1)–N(2)	1.394(2)	C(7)–N(1)	1.365(2)
O(1)–Zn(1)	2.0013(13)	C(9)–N(2)	1.314(2)
O(2)–Zn(1)	2.0726(12)	C(7)–O(1)	1.2583(19)
O(4)–Zn(1)	2.1758(15)	C(11)–O(4)	1.385(3)
O(4)–H(4A)	0.843(10)	C(12)–O(2)	1.259(2)
Zn(1)–O(1A)	2.0013(13)	C(13)–O(3)	1.347(2)
Zn(1)–O(2A)	2.0726(12)	C(16)–O(3)	1.387(3)
Zn(1)–O(4A)	2.1758(15)	C(13)–C(14)	1.324(3)
C(1)–N(1)	1.423(2)	C(14)–C(15)	1.385(3)
Selected bond angles (°)			
C(12)–O(2)–Zn(1)	128.50(12)	O(1A)–Zn(1)–O(4A)	88.95(6)
C(11)–O(4)–Zn(1)	125.29(16)	O(1)–Zn(1)–O(4A)	91.05(6)
Zn(1)–O(4)–H(4A)	115.9(17)	O(2)–Zn(1)–O(4A)	89.48(6)
O(1A)–Zn(1)–O(1)	180.0(12)	O(2A)–Zn(1)–O(4A)	90.52(6)
O(1A)–Zn(1)–O(2)	87.67(5)	O(1A)–Zn(1)–O(4)	91.05(6)
O(1)–Zn(1)–O(2)	92.33(5)	O(1)–Zn(1)–O(4)	88.95(6)
O(1A)–Zn(1)–O(2A)	92.33(5)	O(2)–Zn(1)–O(4)	90.52(6)
O(1)–Zn(1)–O(2A)	87.67(5)	O(2A)–Zn(1)–O(4)	89.48(6)
O(2)–Zn(1)–O(2A)	180.0(12)	O(4A)–Zn(1)–O(4)	180.00(5)

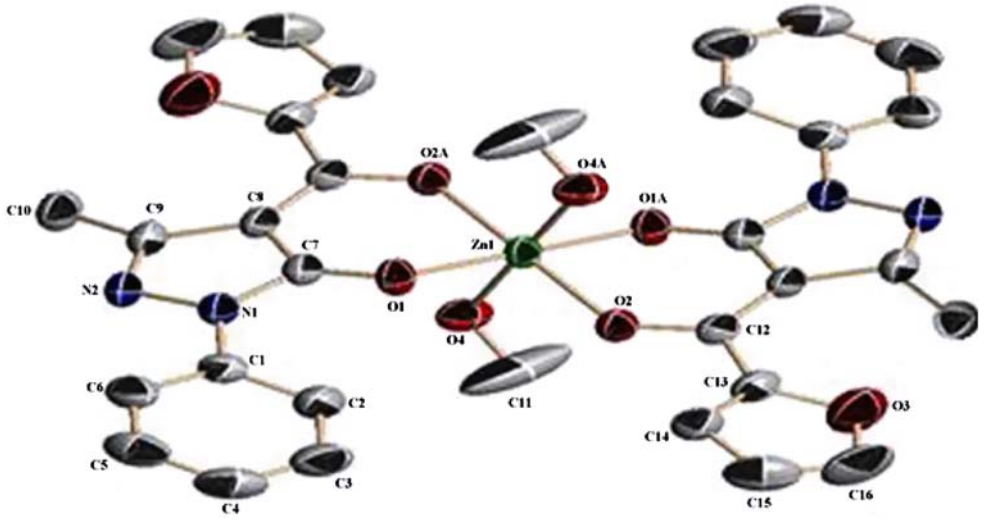

Figure 1. The molecular structure of $Zn(PM\alpha FP)_2(CH_3OH)_2$.

Four oxygens O(2), O(2A), O(1), and O(1A) from two $PM\alpha FP^-$ composed equatorial planes, while two methanols are axial. The angle of O(1A)–Zn(1)–O(1) is 180.00(12)°. The angles of the O(4)–Zn(1)–O(2), O(2)–Zn(1)–O(4A), O(4A)–Zn(1)–O(2A), and O(2A)–Zn(1)–(O4) are 88.95(6)°, 91.05(6)°, 89.48(6)°, 90.52(6)°, respectively; the sum of the angles is 360.00(24)°. Hence, we conclude that the coordination around the Zn is a slightly distorted octahedron.

The C(13)–O(3) bond length is 1.347(2) Å, shorter than 1.43 Å for a C–O single bond and longer than 1.22 Å for a C=O double bond. The C(13)–C(14) and C(14)–C(15) bond lengths are 1.324(3) Å and 1.385(3) Å, respectively, shorter than the C(13)–C(14)

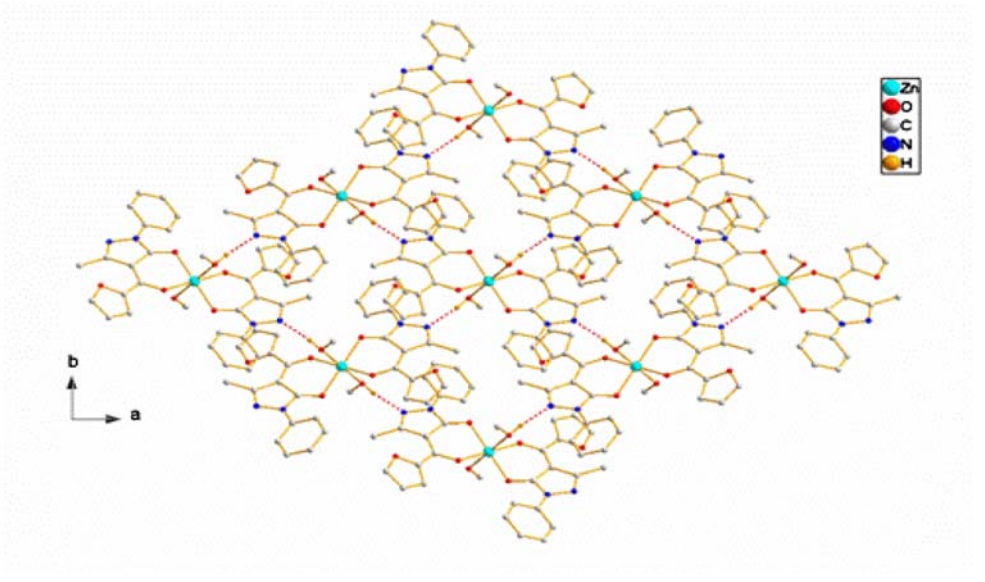

Figure 2. The 2-D network sheet of $Zn(PM\alpha FP)_2(CH_3OH)_2$.

and C(14)–C(15) bond lengths in the free ligand. These changes indicate that during coordination delocalized pyrazolone-ring has averaged the bond length.

Zn(II) and the coordinated oxygens constitute two six-chelate rings which have the boat configuration. All atoms of the chelate and pyrazolone rings lie almost in the same plane. Two methanols connect with the neighboring pyrazolone-ring N(2) through intermolecular hydrogen bonds [O(4)–H(4A)···N(2)] (table 3) [14]. Thus, the [O(4)–H(4A)···N(2)] H-bonding interactions link the 1-D chain motifs into 2-D sheets (figure 2). H-bonding interactions play an important role in forming the supramolecular structure by self-assembly and stabilizing.

3.2. *Spectral analyses*

There are conspicuous differences between the complex and free ligand in IR spectra. In the free ligand, a medium-intensity band at 3011 cm^{-1}, assigned to enol ν(OH) of *β*-diketone tautomer, is absent in complex. A band at 1582 cm^{-1} in the free ligand from ν(C=O) of pyrazolone-ring shifts to 1561.3 cm^{-1} in the complex [15]. The ν(C=C=C) band in the pyrazolone-ring shifts from 1500 to 1477.3 cm^{-1} suggesting coordination through oxygen of carbonyl. The weak band at 495.8 cm^{-1} is related to Zn–O stretch. From these observations, it is concluded that the enolic proton of ligand is replaced by Zn(II) in the complex.

Table 3. Hydrogen bond lengths (Å) and angles (°).

D–H···A	d(D–H)	d(H···A)	d(D···A)	(DHA)
O(4)–H(4A)···N(2)	0.843(10)	1.917(10)	2.757(2)	174(3)

The UV–vis spectrum of the complex in ethanol was recorded from 190 to 900 nm. Three absorptions at 203.2, 275.93, and 305.83 nm are assigned to $\pi \rightarrow \pi^*$ transitions of aryl ring and carbonyl, as well as $n–\pi^*$ transition of carbonyl [16]. The UV spectrum of the complex reflects absorptions of the ligand (λ_{max} (nm) = 203, 235, 279, 310) and three purple-shifted bands emerge. Coordination of Zn(II) and O within the ligand causes polarization of related C=O bond and affects the energy level of the related conjugated molecular orbitals.

Fluorescence properties of the complex and ligand in ethanol were investigated. On excitation at 395 nm, the complex gives a purple emission band at 446 nm assigned to intramolecular fluorescent emission (figure 3). The emission intensity of the Zn(II) complex is much closer to the free Zn emitted at 491–590 nm [17], but the obvious emission for free ligand was not observed. Hence, we conclude that the fluorescence intensity of the

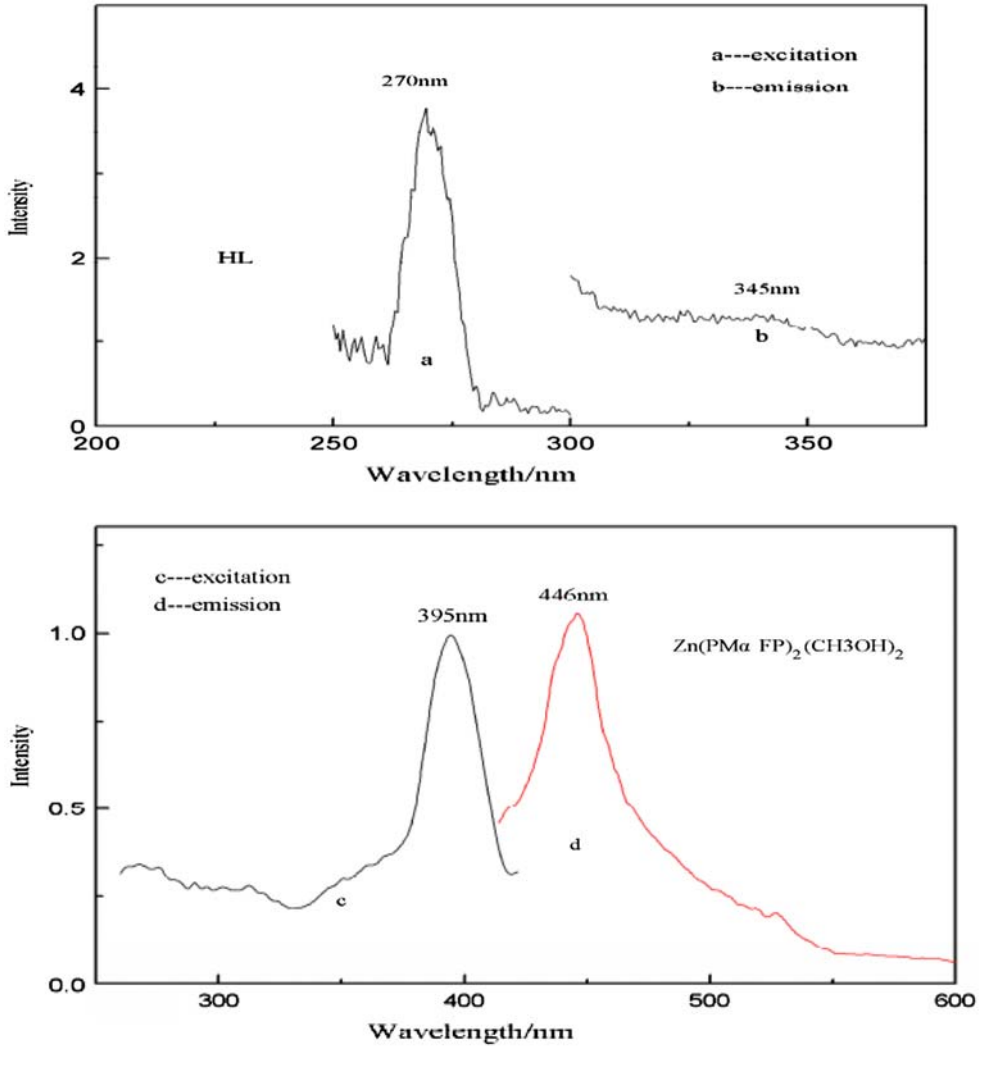

Figure 3. Excitation and emission spectra of ligand and $Zn(PM\alpha FP)_2(CH_3OH)_2$.

Zn(II) complex depends on the free zinc ion. There is a slightly purple shift with respect to free ligand from coordination of Zn affecting energy levels. The fluorescent emission of $Zn(PM\alpha FP)_2(CH_3OH)_2$ suggests that it may be used as a luminescent material.

3.3. *DTA-TG studies*

The DTA-TG curves of $Zn(PM\alpha FP)_2(CH_3OH)_2$ indicate decomposition of the complex in three regions. The first region at 390–638 K with mass loss of 9.5% arises from loss of two methanols (theoretical, 9.6%). In this stage, the DTA curve shows an endothermic peak. The second decomposition from 638 to 728 K with a mass loss of 32.2% is close to the theoretical mass loss of two methyls and two –furoyl($-C_5H_3O_2$) (33%) of pyrazolone rings. In this stage, the DTA curve displays an exothermic peak at 703 K. The last step occurs at 728–851 K, accompanied by an exothermic peak at 778 K in the DTA curve, due to the residue of the complex stepwise decomposing. We conclude the final product is ZnO.

3.4. *Electrocatalytic property*

3.4.1. Preparation of modified GCE. Prior to modification, the bare GCE was polished successively with 0.05 μm Al_2O_3 slurry on the polishing cloth and then rinsed with double-distilled water. After being cleaned, it was scanned by cyclic voltammetry until a reproducible voltammogram was obtained (about 10 min). The electrode pretreated was put in pure water for standby. Putting the electrode pretreated into system: PBS of pH 7.0 containing $1.0 \times 10^{-5}\,mol\,L^{-1}$ title complex stock solution with three electrodes connected with the electrochemistry system, controlling the scan rate at $100\,mV\,s^{-1}$, and scanning potential range in 0.6–1.6 V. The yellow polymer film was obtained by cyclic scanning 12 cycles (the continuous CV of polymerization process: shown in Supplementary material). Capabilities of $Zn(PM\alpha FP)_2(CH_3OH)_2$ prepared in these conditions were very steady; the properties of modified electrode had no evident changes after putting in phosphate buffer solution (PBS, pH = 7.0) after three weeks.

3.4.2. Electrocatalytic behavior of adenine on $Zn(PM\alpha FP)_2(CH_3OH)_2$. The electrocatalytic behavior of adenine was studied with figure 4 depicting the CV of $1.0 \times 10^{-3}\,mol\,L^{-1}$ adenine in pH 7.0 PBS with three different working electrodes. At the bare GCE (figure 4(a)), it can be seen that an irreversible oxidation peak appeared at 1.16 V. At the HPMαFP/GCE (figure 4(b)), the oxidation peak located at 1.11 V negatively shifted 0.05 V and the oxidation peak current (Ipa) increased. However, in the case of $[Zn(PM\alpha FP)_2(CH_3OH)_2]$/GCE (figure 4(c)), the peak current signal of adenine enhanced significantly with the oxidative potential moving negatively compared with the HPMαFP/GCE (ΔEpa is 0.04 V). The above results indicate that the Zn complex in the modified electrode showed good electrocatalytic ability. This phenomenon was probably due to the hydrogen bond between adenine and $PM\alpha FP^-$ of complex, as well as the electropositive Zn^{2+}, which remarkably increased the accumulation amount of adenine [18].

3.4.3. Effect of pH. Influence of pH on electrochemical behavior of $1.0 \times 10^{-3}\,mol\,L^{-1}$ adenine at $[Zn(PM\alpha FP)_2(CH_3OH)_2]$/GCE was investigated from pH 3.0 to 8.0 (see figure 5). With increase of the solution pH, the oxidation peak current of adenine at the modified

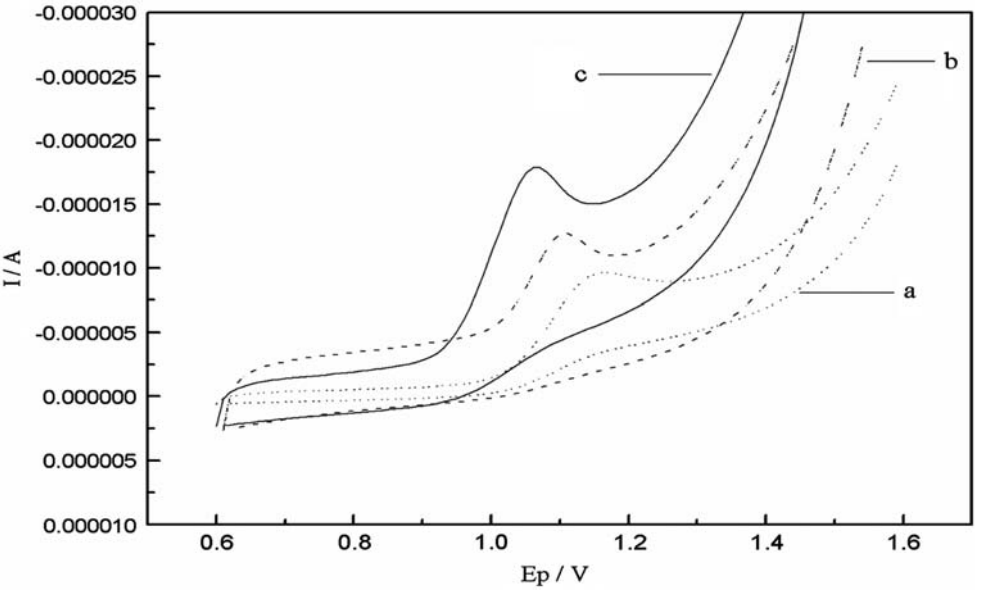

Figure 4. CV of 1.0×10^{-3} mol L^{-1} adenine (pH = 7) at (a) bare GCE, (b) HPMαFP/GCE, (c) $[Zn(PM\alpha FP)_2(CH_3OH)_2]$/GCE. Scan rate, 100 mV s^{-1}.

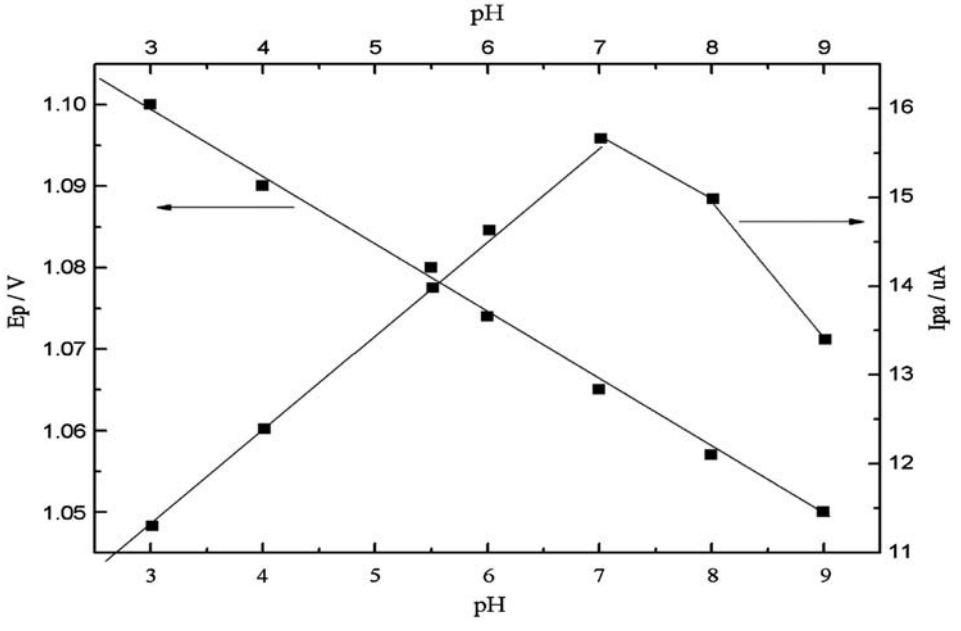

Figure 5. Influence of pH on the peak current (Ipa) and peak potential (E_p) of adenine.

electrode decreased slightly. The pH dependence of oxidation peak potential obeyed the equation, $E_p(V) = 1.289–0.062$ pH ($r = 0.998$). The oxidation of adenine was shown to follow a three-step mechanism involving the total loss of six electrons (shown in scheme 2) and the

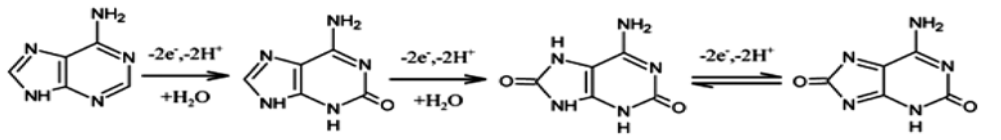

Scheme 2. The reaction mechanism for adenine.

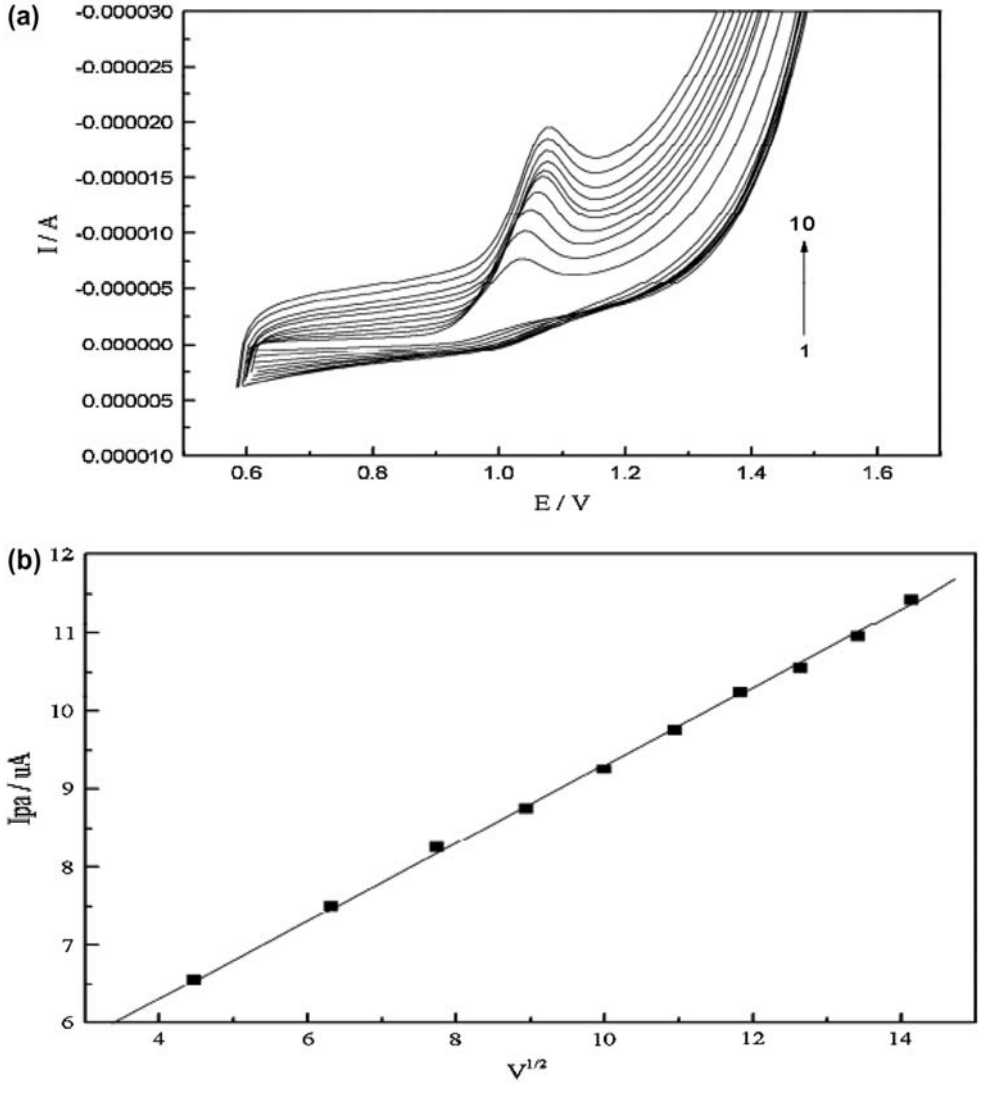

Figure 6. (a) CV of 1.0×10^{-3} mol L^{-1} adenine in pH = 7.0 at various scan rate 20 to 200 mV s^{-1}. (b) Linear relationship plot of the Ipa vs. v.

first 2e$^-$ loss was rate-determining. The slope of 62 mV/pH also indicated that two protons took park in the rate-determining step [19]. This result was in agreement with the electro-oxidation mechanism reported [20–22]. pH values around 7.0 should provide the highest

oxidation currents justifying the selection of pH 7.0 for the subsequent experiments using the modified electrode.

3.4.4. Effect of sweep rate. The effect of scan rate on the voltammetric response for the oxidation of $1.0 \times 10^{-3}\,\mathrm{mol\,L^{-1}}$ adenine on $[Zn(PM\alpha FP)_2(CH_3OH)_2]$/GCE was investigated at pH 7.0. As shown in figure 6(a), along with the increase of the scan rate, the oxidation peak currents of adenine increased gradually. The Ipa and v showed a good linear relationship in the range 0.6–1.6 $\mathrm{V\,s^{-1}}$ (figure 6(b)) with the equation $\mathrm{Ipa}(\mu A) = 4.3598 + 0.4941 v^{1/2}$ ($r = 0.9989$). Such behavior revealed that oxidation of adenine on the surface of $[Zn(PM\alpha FP)_2(CH_3OH)_2]$/GCE was diffusion controlled [23].

4. Conclusions

We have prepared a new furoylpyrazolone Zn(II) complex. The result shows that Zn assumes a slight distorted octahedral MO_6 coordination geometry. The complex exhibits a two-dimensional network structure by intermolecular hydrogen bonds. Fluorescence intensity of the complex depends on free zinc ion. The modified electrode $[Zn(PM\alpha FP)_2(CH_3OH)_2]$/GCE has been used to investigate the electrocatalytic oxidation of adenine. The oxidation of adenine followed a three-step mechanism involving the total loss of six electrons and six protons. The reaction of adenine on the surface of electrode was adsorption controlled. The title complex may be used as a new luminescent and electrochemical material.

Supplementary material

Crystallographic data (excluding structure factors) for the structures reported in this paper have been deposited with the Cambridge Crystallographic Data Center. The CCDC reference number is 774817. Copy of this information may be obtained, free of charge, from The Director, CCDC, 12 Union Road, Cambridge, CB2 IEZ, UK (Fax:+44 1223-336033; E-mail: deposit@ccdc.cam.ac.uk).

Acknowledgments

This work was supported by grants from the Nature Science Foundation of Heilongjiang Province, People's Republic of China (No. B201004).

References

[1] W. Mickler, E. Uhlemann. *Sep. Sci. Technol.*, **20**, 1913 (1993).
[2] M.S. Nagar, P.B. Ruikar, M.S. Subramanian. *Inorg. Chim. Acta*, **141**, 309 (1988).
[3] J.P. Shukla, A.K. Sabnis, M.S. Subramanian. *Thermochim. Acta*, **84**, 207 (1985).
[4] D. Zhang, J.Z. Li. *Anal. Lett.*, **41**, 2832 (2008).
[5] F. Marchetti, C. Pettinari, R. Pettinari. *Coord. Chem. Rev.*, **249**, 2909 (2005).
[6] S. Parihar, S. Pathan, R.N. Jadeja, A. Patel, V.K. Gupta. *Inorg. Chem.*, **51**, 1152 (2012).
[7] Z.Y. Yang. *Synth. React. Inorg. Met. -Org. Chem.*, **32**, 903 (2012).
[8] X.Y. Xie, L. Liu, D.Z. Jia, J.X. Guo, D.L. Wu, X.L. Xie. *New J. Chem.*, **33**, 2232 (2009).
[9] J.M. Li, J.Z. Li, H.Q. Zhang, L.Y. Xu. *Inorg. Chem. Commun.*, **13**, 573 (2010).
[10] J. Li, J.Z. Li, H.Q. Zhang, Y. Zhang, J.Q. Li. *J. Coord. Chem.*, **62**, 2465 (2009).
[11] Y. Song, J.Z. Li. *J. Solid State Electrochem.*, **16**, 689 (2012).
[12] J.Z. Li, W.J. Yu, X. Chin. *J. Appl. Chem.*, **14**, 98 (1997).

[13] G.M. Sheldrick. *Acta Cryst.*, **A64**, 112 (2008).
[14] H.Z. Xu, Y.Q. Zhu, X. Zhang, H.L. Zhu. *Acta Cryst.*, **E60**, 96 (2004).
[15] E.C. Okafo. *Spectrochim. Acta, Part A*, **37**, 945 (1981).
[16] A.B.P. Lever. *Inorganic Electronic Spectroscopy*, Elsevier, Amsterdam (1984).
[17] J.A. Dian, Analytical Chemistry Hankbook, Science (2003).
[18] Y. Song, J.Z. Li. *Instrum Sci. Technol.*, **39**, 261 (2011).
[19] H.Y. Liu, G.F. Wang, D.L. Chen, W. Zhang, C.J. Li, B. Fang. *Sens. Actuators, B*, **128**, 414 (2008).
[20] R.N. Goyal, S. Chatterjee, S. Bishnoi. *Electroanalysis*, **21**, 1369 (2009).
[21] R. Zhang, G.D. Jin, X.Y. Hu. *J. Solid State Electrochem.*, **13**, 1545 (2009).
[22] Z.H. Wang, S.F. Xiao, Y. Chen. *Electroanal. Chem.*, **589**, 237 (2006).
[23] W. Sun, Y.Z. Li, H.W. Gao, K. Jiao. *Microchim. Acta*, **165**, 313 (2009).